Biblid: 0354-9496(2009) 14:1, p.99-104 Naučni rad
UDK: 633.12:631.354 (497.115-17) Scientific paper

NUMERICAL FLOW COMPUTATION OF FLUID MIXING

*Mladenovic N, Markovic D**

SUMMARY

Influence of lateral injected stream, perpendicular to the axis of regular conical nozzle with circular cross section, is analyzed both in subsonic and transonic three-dimensional, turbulent, viscous flows. Turbulence effects are introduced by the formulation based on turbulent kinetic energy. Influence of second fluid component will be analyzed by the application of volume of fluid mixing model. Application in development of machines and equipment for food industry was also analyzed.

Key words: Finite volume method, turbulence, viscosity

1. THEORETICAL POSTULATION

1.1. Conservative Form of the Navier–Stokes Equations

Referring to [1], [2], [3], [4] and [5] the equations can be written as follows:

$$\frac{\partial}{\partial t}\begin{vmatrix}\varrho\\ \varrho\mathbf{v}\\ \varrho E\end{vmatrix}+\nabla\cdot\begin{vmatrix}\varrho\mathbf{v}\\ \varrho\mathbf{v}\otimes\mathbf{v}+p\bar{\bar{\mathbf{I}}}-\bar{\bar{\tau}}\\ \varrho\mathbf{v}H-\bar{\bar{\tau}}\cdot\mathbf{v}-k\nabla T\end{vmatrix}=\begin{vmatrix}0\\ \varrho\mathbf{f}_e\\ \varrho\mathbf{f}_e\cdot\mathbf{v}+q_H\end{vmatrix}, \tag{1.1.1}$$

or

$$\frac{\partial\mathbf{U}}{\partial t}+\nabla\cdot\mathbf{F}_T=\mathbf{Q}. \tag{1.1.2}$$

With the introduction of the total stress tensor $\bar{\bar{\sigma}}=-p\bar{\bar{\mathbf{I}}}+\bar{\bar{\tau}}$, while $\bar{\bar{\mathbf{I}}}$ being unit tensor, one can write the flux vector $\mathbf{F}_T$ as

$$\mathbf{F}_T=\mathbf{F}-\mathbf{F}_v=\begin{vmatrix}\varrho\mathbf{v}\\ \varrho\mathbf{v}\otimes\mathbf{v}+p\bar{\bar{\mathbf{I}}}\\ \varrho\mathbf{v}H\end{vmatrix}+\begin{vmatrix}0\\ -\bar{\bar{\tau}}\\ -\bar{\bar{\tau}}\cdot\mathbf{v}-k\nabla T\end{vmatrix}=\mathbf{v}\mathbf{U}-\begin{vmatrix}0\\ \bar{\bar{\sigma}}\\ \bar{\bar{\sigma}}\cdot\mathbf{v}+k\nabla T\end{vmatrix}, \tag{1.1.3}$$

and finally the Navier–Stokes equations as

$$\frac{\partial\mathbf{U}}{\partial t}+\nabla\cdot(\mathbf{F}-\mathbf{F}_v)=\mathbf{Q}. \tag{1.1.4}$$

It is assumed that a perfect gas constitutive relation is valid, while a Newtonian fluid is defined

* *Prof. dr Nikola Mladenovic, Faculty of Mechanical Engineering, Univercity of Belgrade, Kraljice Marije 16, 11120 Belgrade 35, nmladenovic @mas.bg.ac.rs*

Prof. dr Dragan Markovic, Faculty of Mechanical Engineering, Univercity of Belgrade, Kraljice Marije 16, 11120 Belgrade 35, dmarkovic@mas.bg.ac.rs

by the two viscosity coefficients λ and μ:

$$\tau_{ij} = \mu(\partial_i v_j + \partial_j v_i) + \lambda(\nabla \cdot \mathbf{v})\delta_{ij}. \quad (1.1.5)$$

For fluids where the Stokes relation $3\lambda + 2\mu = 0$ is valid, the shear stress defined by the equation (1.1.5) becomes

$$\tau_{ij} = \mu(\partial_i v_j + \partial_j v_i) - \frac{2}{3}\mu(\nabla \cdot \mathbf{v})\delta_{ij}. \quad (1.1.6)$$

The temperature T is related to the conservative variable ϱE by the expression

$$T = \frac{1}{c_v}(E - \frac{\mathbf{v}^2}{2}) = \frac{e}{c_v}, \quad (1.1.7)$$

where c_v, E and e are the specific heat under constant volume, total and internal energy per unit mass, respectively. One should have in mind that the term $k\nabla T$ in equations (1.1.1) and (1.1.3) represents the heat conduction flux.

1.2. Boundary Conditions

The *no-slip* condition is expressed by $\mathbf{v} = \mathbf{v}_w$ at solid walls. For the temperature, either the wall temperature is fixed at solid walls $T = T_w$, or the heat flux is determined by the physical conditions $-k\partial T/\partial n = q_w$, where q_w is the wall heat flux. For an adiabatic wall $q_w = 0$.

At a solid boundary with a no-slip condition, the momentum equation projected on the normal direction reduces to $\partial p/\partial n = (\nabla \cdot \bar{\bar{\tau}})_n$, where n refers to the normal direction. For thin shear layers at high Reynolds numbers, this relation can be replaced by the boundary layer approximation $\partial p/\partial n = 0$, which can be used as an acceptable alternative for the pressure boundary condition. Conditions on the normal derivative $\partial \mathbf{v}/\partial n = 0$ and $\partial T/\partial n = 0$, are more appropriate, having in mind that there is no absolute and universal rule for the selection of boundary conditions.

1.3. Mixing Model

The tracking of the interfaces between the components is accomplished by the solution of a continuity equation for the volume fraction of one or more of the components [6]. For the q-th component, this equation has the following form:

$$\frac{\partial \alpha_q}{\partial t} + v_i \partial_i \alpha_q = S_{\alpha q}, \quad (1.3.1)$$

where α_q is the q-th fluid's volume fraction in the computational cell. The source term $S_{\alpha q}$ on the right-hand side of equation (1.3.1) is zero for the volume of fluid model. A nonzero source term should be used for models with mass transfer, cavitation model, etc.

The volume fraction equation will not be solved for the primary component; the primary-component volume fraction will be computed based on the following constraint:

$$\sum_{q=1}^{n} \alpha_q = 1. \quad (1.3.2)$$

The properties appearing in the transport equations are determined by the presence of the

components in each control volume.

In a n-component system, the volume-fraction-averaged density takes on the following form:

$$\varrho = \sum_{q=1}^{n} \alpha_q \varrho_q. \tag{1.3.3}$$

All other properties (e.g., viscosity) are computed in this manner.

1.4. Turbulence Model

The Reynolds averaged Navier–Stokes equations are derived by averaging the viscous conservation equations (1.1.1) over a time interval, chosen to be large enough with respect to the time scale of the turbulence fluctuations

$$\frac{\partial}{\partial t}\begin{vmatrix} \bar{\varrho} \\ \bar{\varrho}\tilde{\mathbf{v}} \\ \bar{\varrho}\tilde{E} \end{vmatrix} + \nabla \cdot \begin{vmatrix} \bar{\varrho}\tilde{\mathbf{v}} \\ \bar{\varrho}\tilde{\mathbf{v}} \otimes \tilde{\mathbf{v}} + \bar{P}\bar{\bar{\mathbf{I}}} - \bar{\bar{\tau}}^T \\ \bar{\varrho}\tilde{\mathbf{v}}\tilde{H} - \bar{\bar{\tau}}^T \cdot \tilde{\mathbf{v}} - (k + k_t)\nabla\tilde{T} \end{vmatrix} = \begin{vmatrix} 0 \\ \bar{\varrho}\mathbf{f}_e \\ \bar{\varrho}\mathbf{f}_e \cdot \tilde{\mathbf{v}} + q_H \end{vmatrix}, \tag{1.4.1}$$

where " ˜ " denotes density-weighted averaged property,

$$\tau_{ij}^T = (\mu + \mu_t)\left[\partial_i \tilde{v}_j + \partial_j \tilde{v}_i - \frac{2}{3}(\nabla \cdot \tilde{\mathbf{v}})\delta_{ij}\right], \quad \text{and} \quad \bar{P} = \bar{p} + \frac{2}{3}\bar{\varrho}\tilde{k}, \tag{1.4.2}$$

while μ_t is a *turbulent eddy viscosity* coefficient, and $\tilde{k}$ is the kinetic energy of the mean flow per unit mass.

Turbulence model for the analysis of the viscous effects of turbulent flow, developed by Prandtl [7], [8], [9]and [10] and Kolmogorov [11] and [12], is used in this approach.

$$\bar{\varrho}\frac{DK}{Dt} = -\frac{\partial}{\partial y}(\overline{\varrho v' K'} + \overline{v' p'}) - \bar{\varrho}\overline{u'v'}\frac{\partial \bar{u}}{\partial y} - \mu \sum_{i,j} \overline{\left(\frac{\partial u_i'}{\partial x_j}\right)^2}, \tag{1.4.3}$$

where $K = \overline{(u'^2 + v'^2 + w'^2)}/2$, while u', v' and w' denote fluctuation velocities, and $\bar{u}$ is the mean flow velocity in x direction.

$$\bar{\varrho}\frac{DK}{Dt} = \frac{\partial}{\partial y}\left(\frac{\mu_t}{\sigma_k}\frac{\partial K}{\partial y}\right) + \mu_t\left(\frac{\partial \bar{u}}{\partial y}\right)^2 - c_D\frac{\bar{\varrho}K^{1.5}}{\ell}, \tag{1.4.4}$$

where σ_k is a Prandtl number for turbulent kinetic energy. The equation (1.4.4) having in mind that $\mu_t = \bar{\varrho}K^{0.5}\ell$, for turbulence in the vicinity of a wall the energy equation reduces to the form

$$\tau^2 = \left(\mu_t \frac{\partial \bar{u}}{\partial y}\right)^2 = c_D \bar{\varrho}^2 K^2, \qquad \text{i.e.} \qquad \frac{\tau}{\bar{\varrho}K} = c_D^{0.5}. \tag{1.4.5}$$

After the elimination of K from the dissipation term by introducing the definition of μ_t, the equation (1.4.5) can be expressed in the form of the equation

$$\tau = c_D^{-0.5}\bar{\varrho}\ell^2\left(\frac{\partial \bar{u}}{\partial y}\right)^2, \tag{1.4.6}$$

which is referred to as a "local-equilibrium" turbulence model.

Additional turbulence models (Spallart-Allmaras, $k-\varepsilon$ based and Reynolds stress models) have been described for practical reasons in [6] and [9].

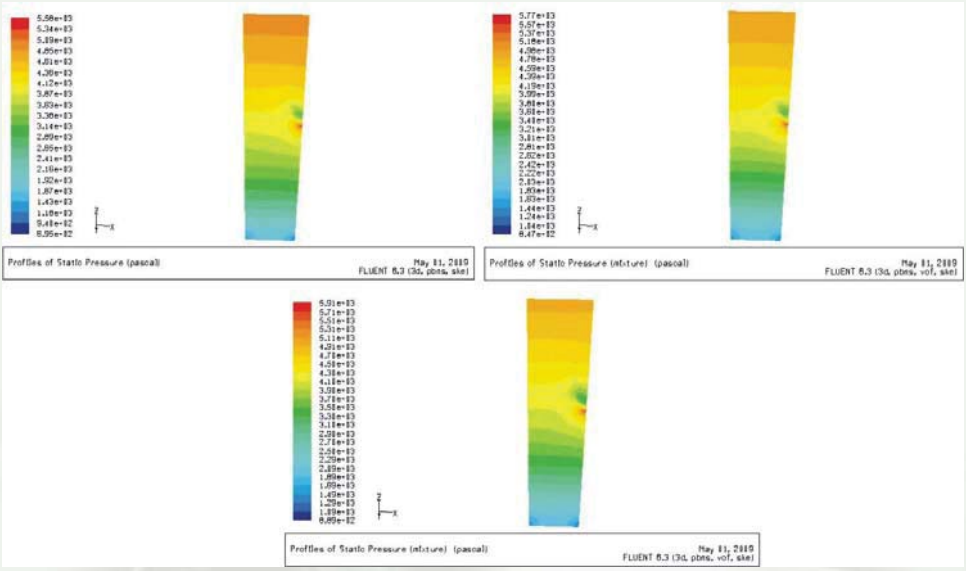

Figure 1. Subsonic Pressure Distribution

2. RESULTS OF NUMERICAL ANALYSIS

Dependence of the main flow properties in divergent regular conical nozzle, with circular cross section, on lateral stream injected perpendicular to the nozzle axis through the circular hole placed on the nozzle wall and located at the half distance between intake and outlet section, has been analyzed. Diameters of the intake and outlet section were $d_i = 0.2\,\mathrm{m}$ and $d_o = 0.3\,\mathrm{m}$, respectively. The injection hole diameter was $d_h = 0.04\,\mathrm{m}$. Finite volume method (**FVM**) has been performed in computation of three-dimensional viscous, turbulent, compressible subsonic and transonic flow of ideal gas. Viscous model, applied in the computation, has been described in the computation, has been described in the section 1.4.

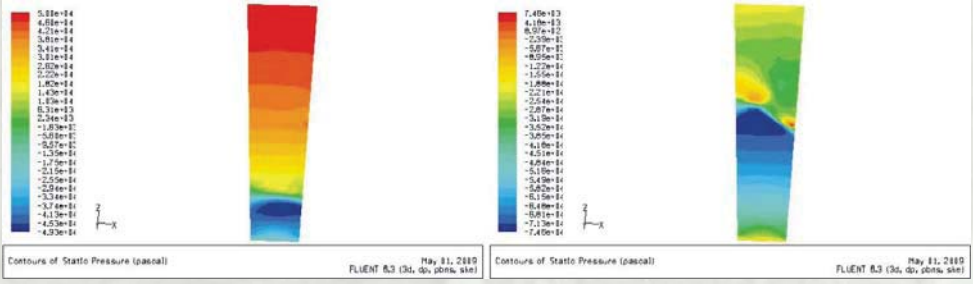

Figure 2. Supersonic Pressure Distribution

Lines of constant pressure in the nozzle symmetry plane in the case of one and two component

subsonic flow have been presented in the Fig.1. In all cases the same boundary conditions have been applied. Flow at inlet section of mass flux $\dot{m}_i = 3.1415\,\mathrm{kg/s}$ has been disturbed by the lateral injection stream $\dot{m}_L = 0.101\,\mathrm{kg/s}$. Uniform pressure distribution of $p_i = 101325\,\mathrm{Pa}$ and stagnation temperature $T_s = 330\,\mathrm{K}$ at the inlet section have been assumed. For the outlet section uniform pressure distribution of $p_o = 97325\,\mathrm{Pa}$ has been prescribed. Calculated pressure distribution of one component air flow has been shown in the Fig.1a, while Fig.1b and Fig.1c illustrate pressure distribution of two component flow with the primary air and secondary oxygen component, and air and hydrogen component, respectively. In both cases fluid's volume fractions were $\alpha_{O_2} = \alpha_{H_2} = 0.3$.

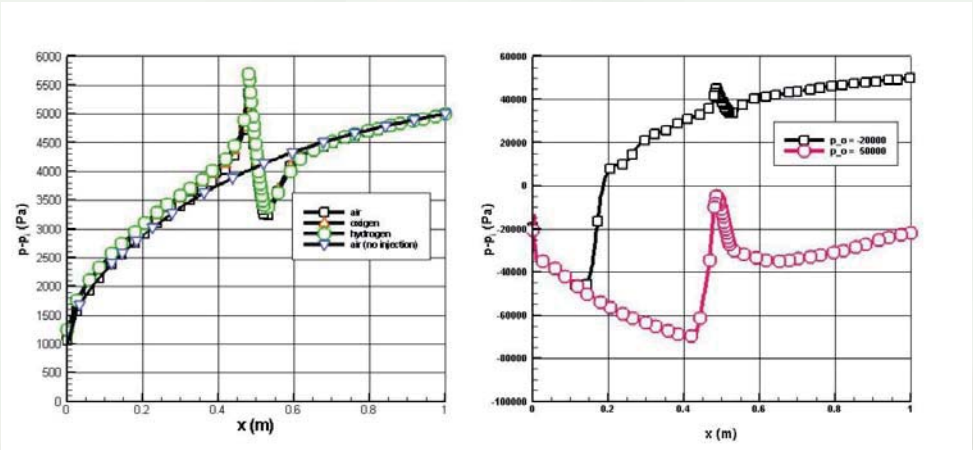

(a) *(b)*

Figure 3. Wall Pressure Distribution

Performed computation has confirmed almost insignificant influence of lateral stream injection on flow separation and pressure distribution $p - p_i$ in all three analyzed cases, compared with main flow without lateral injection, except in the zone close to the injection hole, as can be concluded from the Fig. 3a

Results of analysis for the internal one component transonic air flow are presented in the Fig. 2, for the same nozzle geometry as used in subsonic flow analysis, with inlet mass flux $\dot{m}_i = 12.566\,\mathrm{kg/s}$, lateral injection mass flux $\dot{m}_h = 0.506\,\mathrm{kg/s}$, uniform pressure distribution, both at the inlet and lateral hole section $p_i = p_L = 101325\,\mathrm{Pa}$ and constant stagnation temperature $T_s = 330\,\mathrm{K}$ over the sections. For the first flow case pressure contours in the symmetry plane are shown in the Fig. 2a, for outlet pressure $p_o = 151325\,\mathrm{Pa}$, while for the second case of transonic flow (Fig. 2b) constant value $p_o = 81325\,\mathrm{Pa}$ has been prescribed for the outlet pressure. In the second case, illustrated in the Fig. 2b, the strong oblique shock wave occurs near the location of lateral flow injection and effects of flow separation downstream of the hole position, measured along the nozzle axis, are significantly multiplied, as one can verify from the wall pressure distribution (Fig. 3b).

3. CONCLUSION

Influence of the lateral injected stream, directed perpendicular to the nozzle axis, both in subsonic and transonic, turbulent, viscous, three-dimensional, one and two component flow is analyzed in this paper. Comparison between the results of numerical computation of subsonic one component flow case and "equivalent" (same geometry and boundary conditions) two component flows shows that there is not significant difference in pressure distribution between these cases and flow separation occurs in very limited zone. Numerical analysis, applied to the transonic flow, shows steeper variations of the flow variables, including pressure distribution, than in the subsonic case, having in mind that there is strong influence of the shock wave in the mixing zone. Derived results shown in this paper have potentially wide application in development of new technologies, both in bio-technical systems and in food processing industry.

4. REFERENCES

[1.] Mladenovic N (1992) Transonic Flow Solution of the Thin Layer Navier-Stokes Equations Using Implicir LU factorization, Theoretical and Applied Mechanics, 18, pp. 91-101.
[2.] Hirsch C (1992) Numerical Computation of Internal and External Flows, John Wiley & Sons, Chichester.
[3.] Mladenovic N, Mitrovic Z, Rusov S (2002) Boundary Layer and Shock Wave Interaction in Transonic Flow Computation, Bulletins for Applied and Computer Mathematics, 2015, pp. 327-334.
[4.] Randall J L (2003) Finite Volume Methods for Hyperbolic Problems, Cambridge University Press, Cambridge.
[5.] Versteeg H K, Malalasekera W (2007) An Introduction to Computational Fluid Dynamics – the Finite Volume Method, Person Education Limited, Harlow
[6.] FLUENT INC. (1999) Fluent Reference Manual, FLUENT Corporation, New York
[7.] Prandtl L (1945) Über ein neues Formelsystem für die ausgebildete Turbulenz, Nachrichten von der Akad. der Wissenschaft in Göttingen, Göttingen
[8.] Launder B E, Spalding D B (1972) Mathematical Models of Turbulence, Academic Press, London.
[9.] Shetz J A (1993) Boundary Layer Analysis, Prentice Hall, Englewood Cliffs.
[10.] Patankar S V, Spalding D B (1970) Heat and Mass Transfer in Boundary Layers, Intertext Books, London.
[11.] Kolmogorov A N (1942) Equations of Turbulent Motion of an Incompressible Turbulent Fluid, Izv. Akad. Nauk SSSR, Ser. Phys, 6 (1-2)
[12.] Davidson P A (2005) Turbulence - An Introduction for Scientists and Engineers, Oxford University Press, New York.

The paper received: 03.11.2009. The paper received: 11.11.2009.